Universidad Continental

FACULTAD DE INGENIERÍA

Escuela Académico Profesional de Ingeniería Civil

Tesis

Influence of Vertical Geometric Irregularity on the Seismic Response of High-Rise Buildings Equipped with Base Isolation System

Romel Moises Olivera Perez
Thalia Leticia Julcarima Coca
Lovell Wilder Torpoco Lopez
Manuel Ismael Laurencio Luna

Para optar el Título Profesional de
Ingeniero Civil

Huancayo, 2024

Universidad Continental

INFORME DE CONFORMIDAD DE ORIGINALIDAD DE TRABAJO DE INVESTIGACIÓN

A	:	Decano de la Facultad de Ingeniería
DE	:	Manuel Ismael Laurencio Luna Asesor de trabajo de investigación
ASUNTO	:	Remito resultado de evaluación de originalidad de trabajo de investigación
FECHA	:	19 de Junio de 2024

Con sumo agrado me dirijo a vuestro despacho para informar que, en mi condición de asesor del trabajo de investigación:

Título:
Influence of Vertical Geometric Irregularity on the Seismic Response of High-Rise Buildings Equipped with Base Isolation System

URL / DOI:
https://www.scopus.com/record/display.uri?eid=2-s2.0-85193230188&origin=inward&txGid=cb42f79e7db441e35e826907a77f131c
10.13189/cea.2024.121312

Autores:
1. Romel Moises Olivera Perez – EAP. Ingeniería Civil
2. Thalia Leticia Julcarima Coca – EAP. Ingeniería Civil
3. Lovell Wilder Torpoco Lopez – EAP. Ingeniería Civil
4. Manuel Ismael Laurencio Luna – EAP. Ingeniería Civil

Se procedió con la carga del documento a la plataforma "Turnitin" y se realizó la verificación completa de las coincidencias resaltadas por el software dando por resultado 7 % de similitud sin encontrarse hallazgos relacionados a plagio. Se utilizaron los siguientes filtros:

- Filtro de exclusión de bibliografía — SI [X] NO [ ]
- Filtro de exclusión de grupos de palabras menores — SI [ ] NO [X]
  N° de palabras excluidas **(en caso de elegir "SI")**:
- Exclusión de fuente por trabajo anterior del mismo estudiante — SI [ ] NO [X]

En consecuencia, se determina que el trabajo de investigación constituye un documento original al presentar similitud de otros autores (citas) por debajo del porcentaje establecido por la Universidad Continental.

Recae toda responsabilidad del contenido del trabajo de investigación sobre el autor y asesor, en concordancia a los principios expresados en el Reglamento del Registro Nacional de Trabajos conducentes a Grados y Títulos – RENATI y en la normativa de la Universidad Continental.

Atentamente,

La firma del asesor obra en el archivo original
(No se muestra en este documento por estar expuesto a publicación)

Civil Engineering and Architecture 12(3A): 2091-2115, 2024 http://www.hrpub.org
DOI: 10.13189/cea.2024.121312

Influence of Vertical Geometric Irregularity on the Seismic Response of High-Rise Buildings Equipped with Base Isolation System

Romel Moises Olivera Perez, Thalia Leticia Julcarima Coca, Lovell Wilder Torpoco Lopez*, Manuel Ismael Laurencio Luna

Faculty of Civil Engineering, Continental University, Peru

Received November 7, 2023; Revised March 23, 2024; Accepted April 22, 2024

Cite This Paper in the Following Citation Styles

(a): *[1] Romel Moises Olivera Perez, Thalia Leticia Julcarima Coca, Lovell Wilder Torpoco Lopez, Manuel Ismael Laurencio Luna , "Influence of Vertical Geometric Irregularity on the Seismic Response of High-Rise Buildings Equipped with Base Isolation System," Civil Engineering and Architecture, Vol. 12, No. 3A, pp. 2091 - 2115, 2024. DOI: 10.13189/cea.2024.121312.*

(b): *Romel Moises Olivera Perez, Thalia Leticia Julcarima Coca, Lovell Wilder Torpoco Lopez, Manuel Ismael Laurencio Luna (2024). Influence of Vertical Geometric Irregularity on the Seismic Response of High-Rise Buildings Equipped with Base Isolation System. Civil Engineering and Architecture, 12(3A), 2091 - 2115. DOI: 10.13189/cea.2024.121312.*

Abstract In the year 2022 according to the United Nations, the world population is three times larger than the twentieth century, which affects the demand for land and consequently the cost per m^2 increases. Likewise, it requires occupants to choose to build high-rise buildings to maximize the area acquired, consequently most structures require huge shear walls that increase the cost in steel, and in turn reduce the profitability of real estate for lack of aesthetic spaces on the floors. Now, recent architectural models do not allow regular structures, consequently, different irregularities occur. The present work develops the influence of vertical geometric irregularity in high-rise buildings with base isolation system, by which the researchers, modellers and designers, carried out the analysis of a regular pattern model (MPAT) based on shear walls, columns and beams against 12 different models, presented in their structural configuration different vertical geometric irregularities, consisting of 20 floors. It was analyzed by means of the seismic properties established in the Peruvian regulation of buildings norm E.030 and E0.31, providing with rigidity, resistance, ductility to the structure, likewise the elements of isolation of base of the type Elastomeric LRB and Slider were placed, which were developed with a nonlinear analysis time history with a total of 7 pairs of seismic registrations. Finally, it was observed in the displacement analysis that the irregular structures compared to the regular structure do not present a variation greater than 3.14%. Similarly, drifts between floors were analysed in which the models M1T3, M2T3, M3T3, and M4T3 presented greater drifts compared to the regular model, obtaining in the model M4T3 an increase in the drift of 56. 74%. On the other hand, in the accelerations per level, the M2T3 model obtained an increase of 60.63% compared to the standard model. Finally in the analysis of energy dissipation with seismic isolators, the M4T3 model dissipates 92.84% of energy generated in the structure, consequently the seismic effect is dissipated directly by the base isolators.

Keywords Displacement, Drifts, Acceleration, Vertical Geometric Irregularity, Energy Dissipation, Base Isolation, Seismic Isolation, High-rise Buildings

1. Introduction

According to the National Institute of Statistics and Informatics (INEI), in 2023 the Peruvian population will reach 33 million 726 thousand inhabitants, of which 30.1%

live in Metropolitan Lima [1]. These statistics involve the real estate sector caused by the modern city, i.e. the expansion of buildings is part of the commercial and residential districts. Likewise, Lima's population prefer the flats located on the highest floors because of the privileged view, in fact they are the first to be marketed [2]. Tall buildings in Lima are exposed to seismic movements throughout their useful life because they are within the Pacific Ring of Fire that concentrates the highest seismic activity in the world with the possibility of generating an earthquake of a great magnitude [3], for this reason the structure must control the displacements that are generated in the floor levels to avoid collapse and to maintain immediate occupancy safety [4]. Thanks to the progress of earthquake-resistant engineering, measures have been taken to reduce the seismic demand on structural elements through the isolation of LRB and Slider isolators, which improve the dynamic behaviour of the structure [5]. Additionally, there are other components that influence structural damage such as vertical geometric irregularity that punishes the basal shear by an increase of 11.11% directly affecting displacement, accelerations, drifts, increased steel requirement in beams, columns, plates [6].

The Turkish Department of Architecture has conducted a comprehensive analysis of seismic events in Turkey. In 1999, a devastating earthquake with a magnitude of 7.4 claimed the lives of more than 17,000 people and left more than 280,000 homes destroyed [7]. In addition, in 2023, another 7.8-magnitude earthquake struck the region, resulting in the loss of 4,300 lives and the collapse of numerous buildings, as illustrated in Figure 1, labelled A). In Mexico, the 15-storey Nuevo Leon building collapsed during the 1985 earthquake, which reached a magnitude of 8.1, leaving a tragic toll of 300 people dead in its collapse. This tragedy is highlighted in Figure 1, identified as B) [8]. On the other hand, in Chile, significant seismic events have been recorded, such as the Valparaíso earthquake in 1985, with a magnitude of 8, and the Maule earthquake in 2010, with a magnitude of 8.8. These events affected large areas, including the metropolitan region and Valparaíso, as well as areas such as Viña del Mar, where collapses of structures have been reported, as shown in Figure 1, marked C) [9].

It is evident from Figure 1 that some tall office buildings focused their efforts on structural stiffness, but did not incorporate seismic isolation systems, which contributed to their collapse.

In Peru, the introduction of base isolation is a relatively new measure in terms of seismic protection. Currently, this approach is being used mainly in hospitals, although in its early days, its application was carried out using foreign codes due to the absence of local regulations. This has raised concerns about the adequacy of these isolated buildings to accurately resist the country's own seismicity [10]. In addition to its implementation in hospitals, base isolation has been used in other structures in Peru, such as the municipality of Moquegua and UTEC University. It has also been applied in bridge construction. Moreover, in 2014, the Peruvian government established that all public health centers should be built with base isolation [11]. Despite these advances, it is important to continue developing local regulations and standards that are specifically adjusted to the seismic characteristics of Peru, thus ensuring the effectiveness and safety of isolated structures in the country.

A) Collapsed buildings in Turkey earthquake 2023 B) Building collapse Nuevo león 1985 quake C) Building collapse Maule earthquake 2010

Figure 1. Collapse of buildings in different countries due to seismic events

In Turkey, isolated and fixed base models were carried out, in which the behaviour of the lead rubber bearing (LRB) was evaluated against flat slider isolation systems (FS), curved surface friction (FPS) for low and medium height buildings, in which 352 analyses were carried out, in the non-linear range, The behaviour of the models without a base isolation system was evaluated. They obtained a higher seismic requirement exceeding the state of controlled damage; on the other hand, the lateral displacements of the isolated models were higher. The researchers concluded that the joint use of the LRB and FS isolator is detrimental to the behaviour of the structure by increasing the seismic demand, while the use of the LRB isolator alone is detrimental because the FS isolator lacks a restoring force, as opposed to the LRB devices that do produce a restoring force. It is concluded that the use of the LRB isolator is a better option than other base isolation systems [12]. On the other hand, the researchers [13], evaluated the base isolation with elastomeric support constituted of rubber with lead core (LRB), in which they considered effects of torsional irregularity and 1408 different time history analyses. They have used the three-dimensional models of 3,5,7, 9 storey models using 11 records obtained from the ground, demonstrating sensitive behaviour to torsional irregularity effects, affecting 47% higher than a model without eccentricity. One of the factors to this result is that the lack of seismic records leads to inaccurate predictions of seismic demands.

In Italy, the behaviour of irregular and asymmetric structures was analysed, this induces the structure to generate seismic overload actions on the elements distributed around the frames, generating a fragile behaviour; To reduce this vulnerability, they proposed structuring strategies, through the addition of shear walls, structural frames, elastomeric base isolation. The latter solution is intended to be more effective because it reduces vulnerability due to irregularity, in which it has been demonstrated that the isolated system allows to reduce the total shear stress of the base by 70% by decoupling the vibration modes in an adequate way in order to obtain 2 translations in the first modes and in the third one torsional mode. This characteristic allows to distribute the stresses in the columns in a uniform way avoiding dynamic loads in the surroundings of the columns and avoiding forced torsional effects [14]. On the other hand, in multi-storey tall buildings characterised by irregularity in plan, they were analysed by means of response spectrum analysis and non-linear analysis, demonstrating that an analysis carried out with the response spectrum provides lower drift values, and consequently in dynamic analysis it is less conservative compared to the non-linear analysis, in terms of displacement. In the same way, the forces generated in the beams and columns with respect to the bending moment were evaluated, generating lower values in a response spectrum compared to the non-linear analysis, while in a shear analysis in the supports they are very similar, which is why the researchers recommend using a non-linear analysis in irregular multi-storey buildings with base isolation systems [15-16].

Experimental studies in the United States on elastomeric insulation evaluated its behaviour under shear deformation to predict what happens under seismic stresses, with the axial load being decisive during design. This is calculated under the Haringx theory, based on small displacements and modified by a correction factor to take into account shear effects. In this study, it is shown that the critical load decreases as the horizontal displacement or the shear deformation generated increases. It is also shown that the formulae used for the design are not conservative for small displacements, but for large displacements, they are too conservative [17].

In the Asian continent they evaluated high-rise buildings using base isolation which is accepted for seismic design, where it is mentioned that the elastomeric isolator is the most used. But still there is a tendency of the friction pendulum bearing (FPB) due to its high vertical bearing capacity, which has been developed with a non-linear analysis obtaining a base response, under wind load a non-zero mean by linearisation. Finally the research mentions that the effects of radius and coefficient of friction are induced to the vibration generated by the wind, offering guidelines for design of tall buildings affected by wind [18].

The effectiveness of viscous fluid dampers (VFD) in combination with floor isolators has been evaluated in China, showing that this combination significantly improves the structural performance of buildings by reducing floor drifts and shear force. However, finding the optimal parameters for VFD can be challenging. Although the use of viscous fluid dampers together with isolators is common in buildings close to earthquake faults, this hybrid system is also advantageous in inter-storey isolation to limit P-Δ effects. However, previous research on base isolation has pointed out that this additional damping can have negative effects by increasing inter-storey drifts and floor accelerations [19] [20].

This background provides clear guidelines for the isolation of tall buildings using elastomeric isolators, ruling out the use of viscous fluid dissipators due to their negative effects on floor drifts and accelerations. Furthermore, it is recognised that these effects can be aggravated when considering geometric irregularity, which is the focus of this research. Therefore, our aim is to improve the structural behaviour by means of isolators, focusing on analysing only the vertical geometric irregularity as the main variable. For this purpose, it has been considered essential to carry out a modelling with a non-linear analysis. In this study, four different types of models will be evaluated, each with three variations, involving the analysis of 12 different configurations of vertical geometric irregularity. These configurations will be tested using a base isolation system composed of LRB elastomeric isolators in conjunction with Slider type isolators. Various parameters such as displacements,

accelerations, drifts and energy dissipation will be studied in comparison with a regular isolated building in order to better understand the behaviour of the structure under seismic conditions.

2. Materials and Methods

In this study, theoretical concepts were used to analyse the behaviour of the structure, establishing a relationship between the independent variable, the vertical geometric irregularity, and the dependent variables, such as the LRB and Slider base seismic isolator.

2.1. Seismic Properties of the Structure

The seismic properties are requirements to evaluate the behaviour of the structure, which are governed according to the Peruvian building regulation Norma E.030 Diseño Sismorresistente [21]. In relation to zoning, the project is located in Lima, therefore, the zoning parameter (Z4=0.45). The use factor for isolated structures is equal to 1 (U=1) [22], the seismic amplification factor (C) is a function of the period of the building and the soil parameters, and the soil factor (S) is a function of the zoning, which depends on the soil study having a shear wave between 500 m/s and 1500 m/s, located in (S1=1). Finally the reduction coefficient of seismic forces (R) in the analysis of seismic records was considered a R=1 for the non-linear analysis time history.

2.2. Computational Modelling in ETABS

ETABS is a structural analysis software used in buildings with seismic isolation systems [22]. The study building, depicted in Figure 2, has a total floor area of 1512 m^2 and consists of 20 floors with a total height of 62.4 m. The configuration of the seismic-resistant system includes a core of reinforced concrete walls, beams, and columns. In addition, it rests on a 1.8 m thick slab, supported by 24 natural rubber isolators, of which 16 incorporate a lead core. Therefore, isolated footings have been provided for the isolators which are interconnected by foundation beams. The isolated model and the perimeter structures have implemented a 50 cm insulation joint, which significantly exceeds the minimum requirements, in order to minimise the possibility of impact between the isolated structure and the surrounding structures.

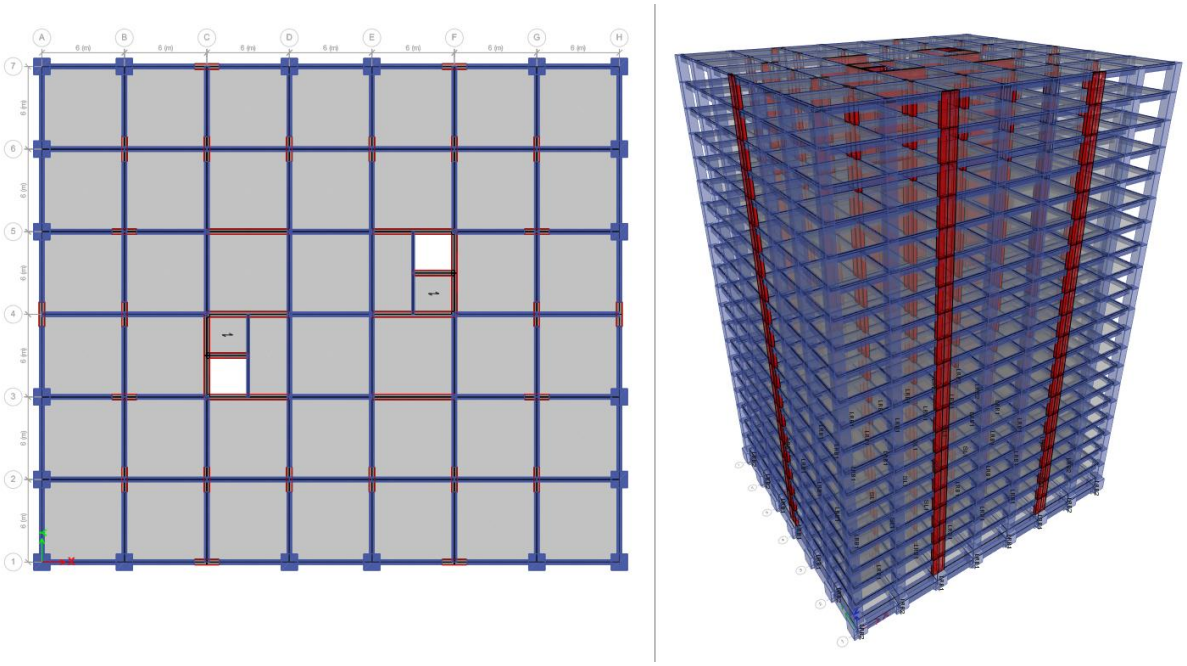

Figure 2. MPAT Computational Model in ETABS of the building

2.3. Building Structuring

The structuring of buildings in Peru is subject to strict requirements of stiffness and resistance established by the Peruvian Building Regulations, specifically in Standard E.031 [22], which limits drifts and accelerations at all floor levels. Therefore, in the analysis of vertical geometric irregularity, it was chosen to use models that include beams, columns and shear walls, as shown in Table 1. Square columns measuring 1.2 m were utilized with a concrete resistance of 420 kg/cm ² from the first to the tenth floor. From the eleventh to the fifteenth floor, the column geometry was reduced to 1.1 m with a compressive strength of 350 kg/cm ², then from floor 16 to 20 the column dimension is 1 m with a concrete of 280 kg/cm^2, the concrete walls in their totality maintained a constant thickness of 0.4 m, and the floor slab elements were maintained at 0.2 m while the beams were 0.35 m wide and a camber of 0.6 m. This gives us an idea regarding the requirement of axial compressive strength decreases as one ascends at the upper levels.

In Figure 3, we visualise the elevation of the structure with mezzanine levels of 3 m, foundation slab of 1.8 m, isolated foundation height of 3.1 m, having a total of 20 storeys, whereby the columns have a variation in compressive strength as the levels are raised accordingly.

2.4. Vertical Geometric Irregularity

The vertical geometric irregularity, according to the Peruvian Technical Standard E.030 [23], refers to a particularity in the spatial configuration of buildings that affects their response to seismic events. This irregularity is vertical when the horizontal dimension of the system of resistance to lateral forces at a specific level exceeds by 130% or more the dimension of the level immediately below. Likewise, the Colombian Seismic Resistant Construction Regulation (NSR-10) establishes the same relationship as the Peruvian standard, which penalises the coefficient of reduction of seismic forces at 0.9. Figure 4 shows 3 configurations to evaluate the vertical geometric irregularity, depending on the total lengths of the cross section versus the corresponding change in length. The irregularity adopted for each configuration is outlined in Figure 5.

Figure 5 shows the 12 structural configurations with vertical geometric irregularity, where the irregularities were evaluated accordingly as indicated in the E.030 seismic-resistant design standard, which was detailed in Figure 3, in which we can highlight that the T3 models are the ones that show an irregularity ratio of 1.75 to 2.33 being higher compared to other irregular models.

Table 1. Geometric properties of the structure

COLUMNS AND WALLS			BEAM AND SLAB			
FLOOR 20	F'c=280	C100X100	e=40cm	F'c=280	V35x60	20cm
FLOOR 19	F'c=280	C100X100	e=40cm	F'c=280	V35x60	20cm
FLOOR 18	F'c=280	C100X100	e=40cm	F'c=280	V35x60	20cm
FLOOR 17	F'c=280	C100X100	e=40cm	F'c=280	V35x60	20cm
FLOOR 16	F'c=280	C100X100	e=40cm	F'c=280	V35x60	20cm
FLOOR 15	F'C=350	C110X110	e=40cm	F'c=280	V35x60	20cm
FLOOR 14	F'C=350	C110X110	e=40cm	F'c=280	V35x60	20cm
FLOOR 13	F'C=350	C110X110	e=40cm	F'c=280	V35x60	20cm
FLOOR 12	F'C=350	C110X110	e=40cm	F'c=280	V35x60	20cm
FLOOR 11	F'C=350	C110X110	e=40cm	F'c=280	V35x60	20cm
FLOOR 10	F'C=420	C120X120	e=40cm	F'C=350	V35x60	30cm
FLOOR 9	F'C=420	C120X120	e=40cm	F'C=350	V35x60	30cm
FLOOR 8	F'C=420	C120X120	e=40cm	F'C=350	V35x60	30cm
FLOOR 7	F'C=420	C120X120	e=40cm	F'C=350	V35x60	30cm
FLOOR 6	F'C=420	C120X120	e=40cm	F'C=350	V35x60	30cm
FLOOR 5	F'C=420	C120X120	e=40cm	F'C=350	V35x60	30cm
FLOOR 4	F'C=420	C120X120	e=40cm	F'C=350	V35x60	30cm
FLOOR 3	F'C=420	C120X120	e=40cm	F'C=350	V35x60	30cm
FLOOR 2	F'C=420	C120X120	e=40cm	F'C=350	V35x60	30cm
FLOOR 1	F'C=420	C120X120	e=40cm	F'C=350	V35x60	30cm
ISOLATED SLAB				F'C=420	V100x200	180cm

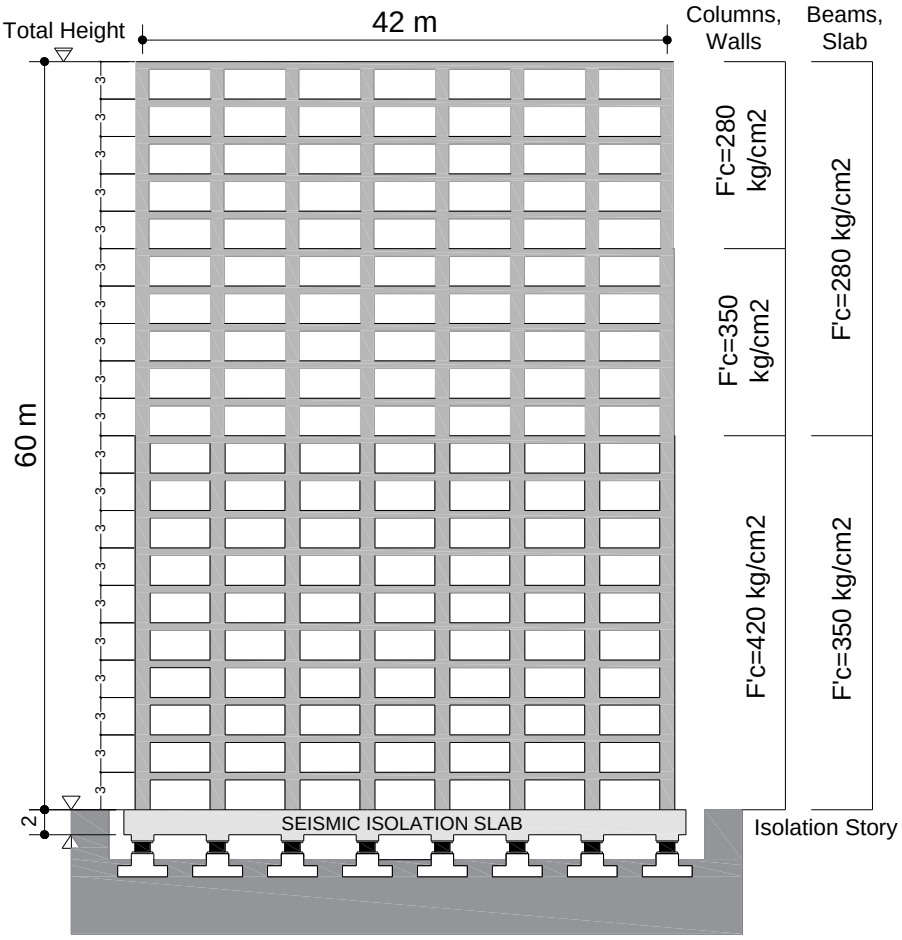

Figure 3. Structuring detail

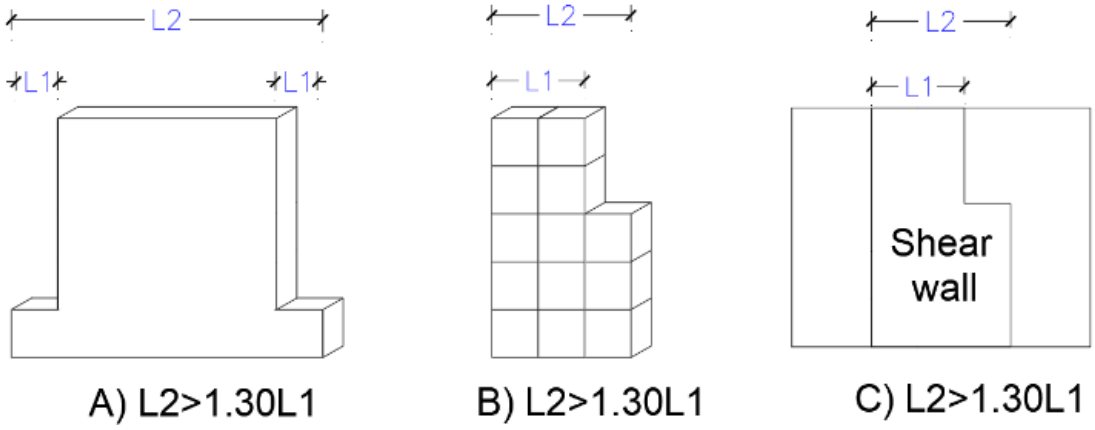

Figure 4. Vertical Geometric Irregularity according to E.030

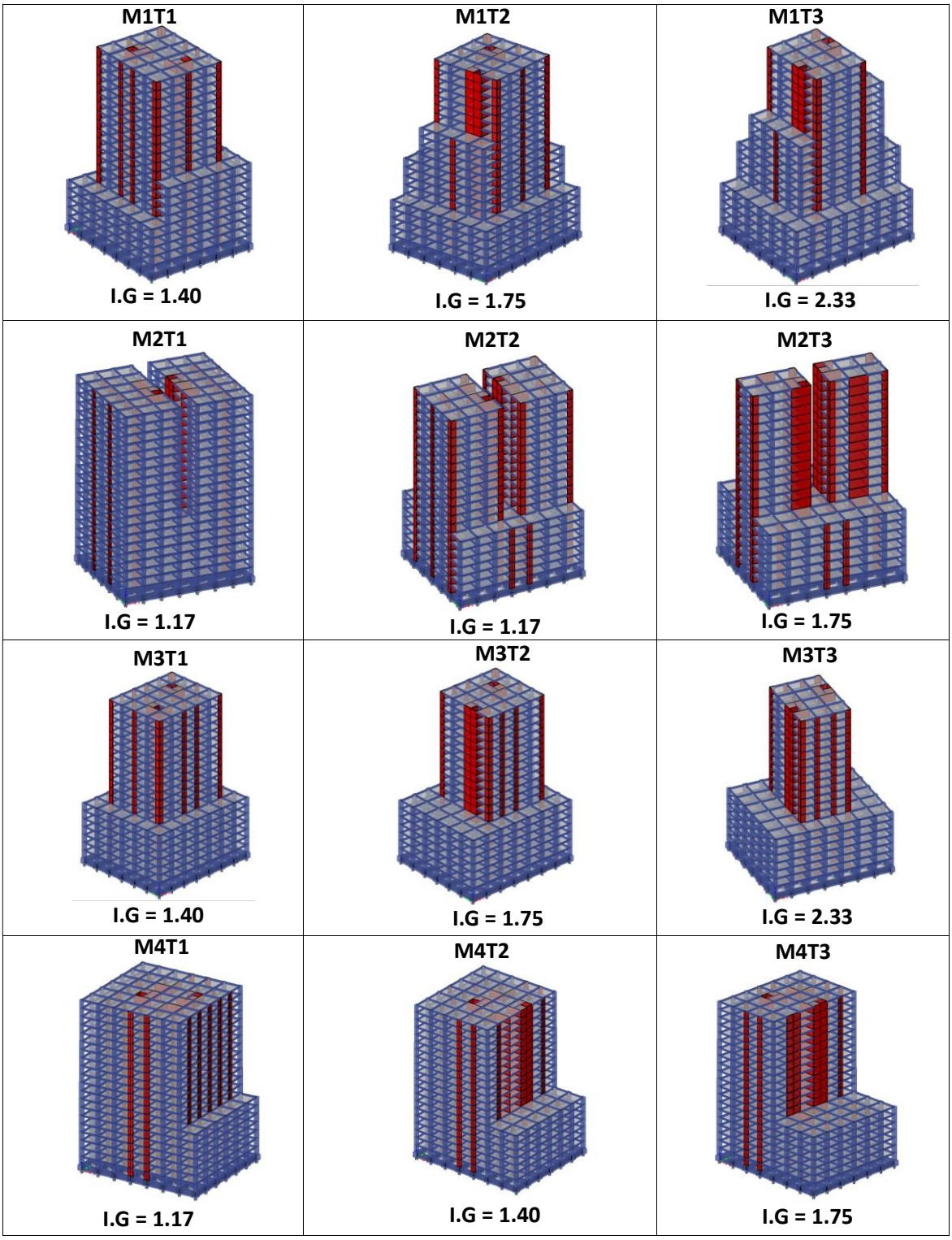

Figure 5. Models with vertical geometric irregularity

2.5. Base isolation System

2.5.1. Dynamic Behaviour of the Isolated Building

Seismic isolation consists of separating a structure from ground motions by coupling flexible elements between the superstructure and foundation [24]. The intention is to reduce the fragility of structures by contributing to damping for deformation control, as well as to shorten displacements between the ground and the building [25]. Figure 6 shows the rigid building moving with base isolators, which decreases seismic amplification and stabilises the building. The flexibility provided by the isolators allows to adapt the ground deformation into a shear deformation, making it difficult to transfer the ground motion to the structure.

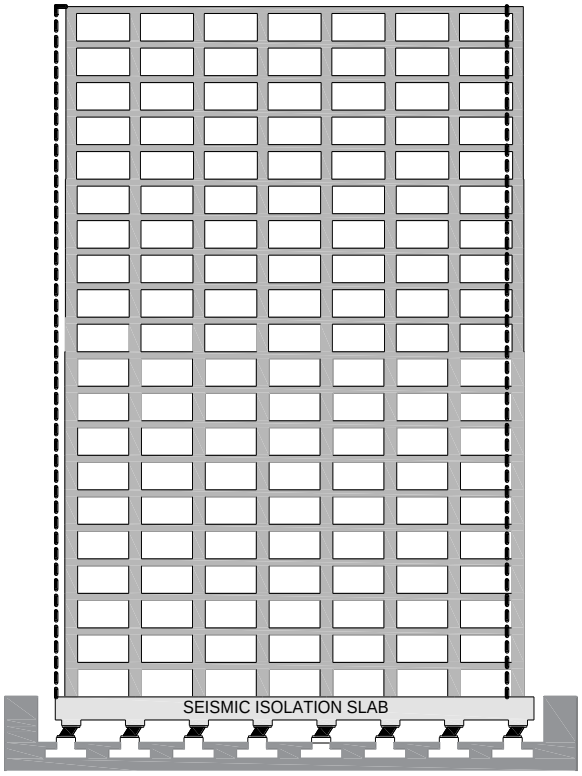

Figure 6. Base-isolated building

2.5.2. Dynamic Behaviour of the Unisolated Building

During a seismic event, ground vibration is transmitted to the buildings through their foundations and consequently transferred to the superstructure. Buildings without seismic isolation are designed to withstand gravity loads, however, in a seismic event the structure resists dynamic loads acting in all directions causing the structural elements to suffer horizontal displacements [26] as shown in Figure 7, the behaviour of the structure without seismic isolation is visualised in which the embedded base is considered generating increased displacements.

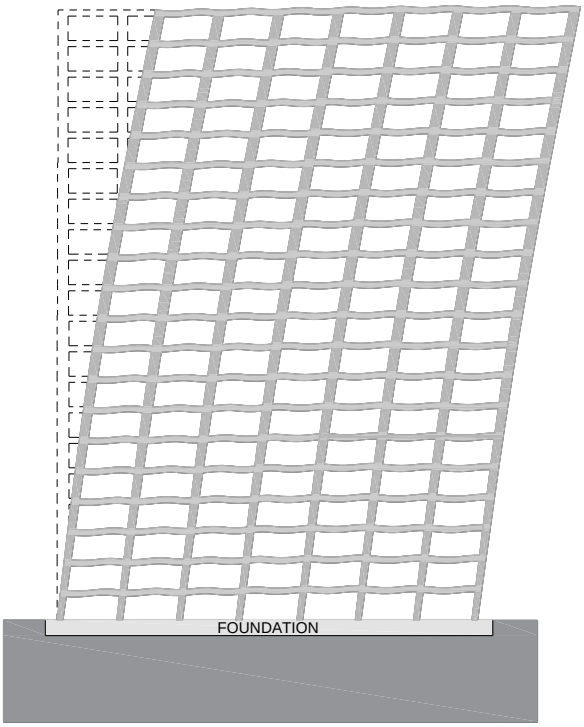

Figure 7. Building without base insulation

2.5.3. LRB Elastomeric Isolators: The Bilinear Model

Lead core bushings (LRB) consist of alternating layers of rubber and A1 steel sheets [27], as shown in Figure 8, with a hole in the centre where the lead core is placed to increase the initial stiffness and energy dissipation capacity [28-29-30]. In addition, an isolation system provides structural safety and lower seismic demand [31]. The details of the LBR isolator are shown in Figure 9, as well as the nominal properties of the bilinear model of the isolator [22].

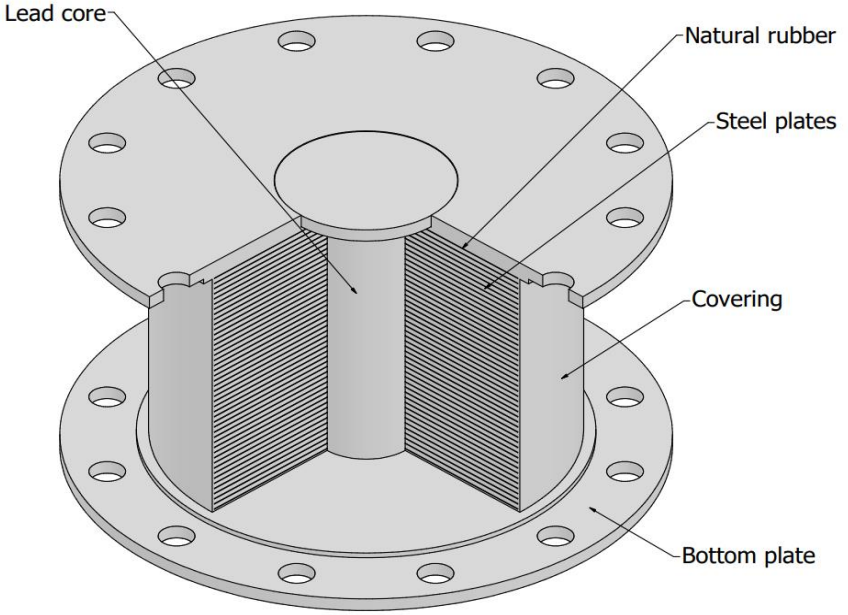

Figure 8. Lead core insulator

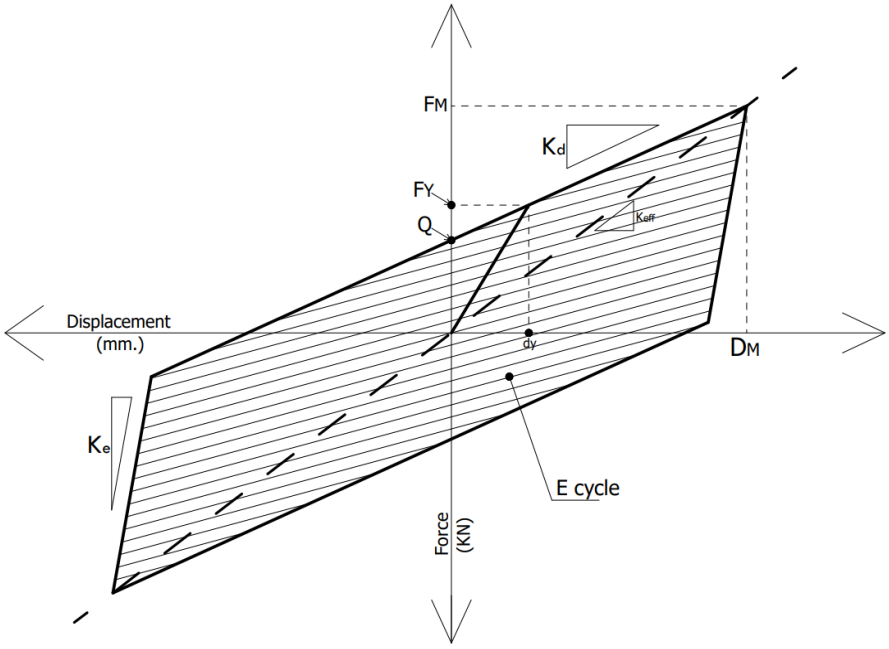

Figure 9. Bilinear force-deformation model of the insulator [22].

In the Bilinear model the post-flow stiffness K_d has to be found for each loading cycle, where G is the shear modulus of the rubber, A_{caucho} is the area of the rubber and F_{max} is the total thickness of the rubber which are given in equation (1) [32].

$$K_d = \frac{G \cdot A_{caucho}}{T_r} \quad (1)$$

Another parameter is the effective stiffness which is found for each load cycle, where F_{max} the maximum force, in D_{max} correspondingly according to equation (2) [29].

$$K_{eff} = \frac{F_{max}}{D_{max}} \quad (2)$$

2.5.4. Slider Isolators: Bilinear Model

Sliding isolators use a sliding surface, usually stainless steel, on which a steel plate coated with Polytetra Fluoroethylene slides and supports the structure as shown in Figure 10; this surface allows horizontal movements independently of the ground. The seismic isolation system is able to dissipate energy through its frictional forces emitted by the earthquake, also this type of isolation may

require other types of seismic isolators (LDRB, LRB or HDRB) to restore the structure to its initial position after the earthquake [33].

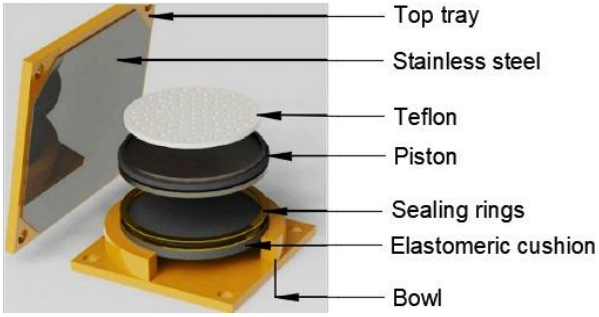

Figure 10. Sliding support

2.6. Acceleration Recording

The acceleration records are the tapes obtained from different stations in order to generate a database with existing information [34], for the analysis of the structure at least seven pairs of ground acceleration records are required consisting of a pair of orthogonal components chosen and scaled from individual events to construct the pseudo-acceleration spectrum taking the square root of the sum of squares (SRSS) [21-22]. Table 2 shows the seven chosen records that were extracted from CISMID for the analysis of the structure, which must be spectrum compatible i.e. they must have similar properties such as soil type.

2.6.1. Effects of Seismic Loads and Design Combinations

The irregular modelling that makes up the isolated structure must use the additional load combinations for the design stage and for testing of the prototype units of the isolation system set out in equation (3), (4), (5) [22].

$$P_{service} = 1.0CM + 0.5CV \quad (3)$$

$$P_{maximo} = 1.25(CM + CV) + 1.0(CSH + CSV) \quad (4)$$

$$P_{minimum} = 0.9\text{CM-}1.0(\text{CSH+CSV}) \quad (5)$$

Where:
CM: Dead Cargo
CV: Live Cargo
CSH: Horizontal Seismic Loading
CSV: Vertical Seismic Loading

2.7. Acceleration Log Processing

The records defined in Table 2 show that most of the stations at the moment of recording a seismic event have disturbances due to factors such as passing cars, trains, ambient noise, etc [35]. This generates a superposition in the initial signal by another signal of a certain level that can hide important features. Thus, it is necessary to correct the accelerations obtained from the Seismosignal recording; Figure 11 shows the correction of the acceleration vs. time of the Lima earthquake in 1966. The blue line represents the baseline correction and the filtering of the data that caused the perturbations, while the lead line represents the initial data without corrections.

Table 2. Seismic records from time-history analysis

Earthquake	Date	Mw	Depth (Km)	PGA (g)	Hypocentral Depth (Km)
Lima, Perú	17/10/1966	8	37.3	0.275	223.1
Chimbote, Perú	31/05/1970	7.9	71.1	0.107	368.3
Lima, Perú	3/10/1974	8.1	21.2	0.196	58.8
Moquegua, Perú	23/06/2001	8.4	29	0.294	325.6
Arequipa, Perú	7/07/2001	7.5	33	0.126	82
Moyobamaba, Perú	25/09/2005	7.5	115	0.134	90
Ica, Perú	15/08/2007	7.9	40	0.494	117

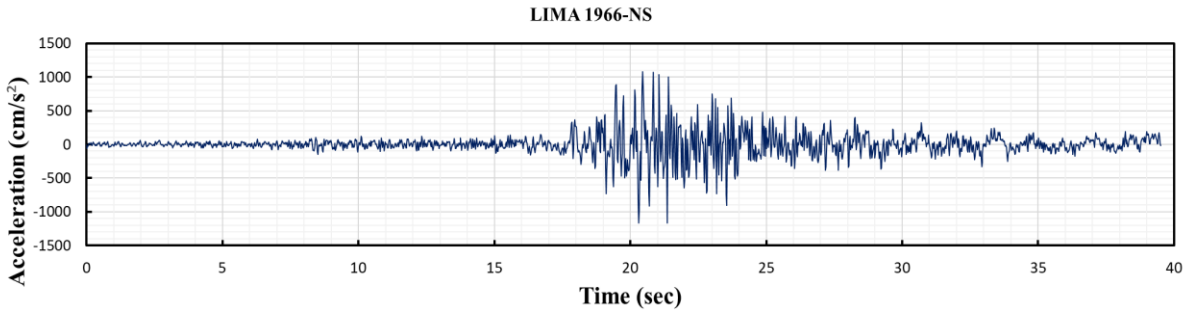

Figure 11. Baseline correction and filtering of the lime register, 1966

Figures 12 and 13 show the seven records scaled to the design spectrum, where a 5% damping of the structure is considered, a seismic reduction factor (R=1), which will later be used for the non-linear time-history analysis of the structure.

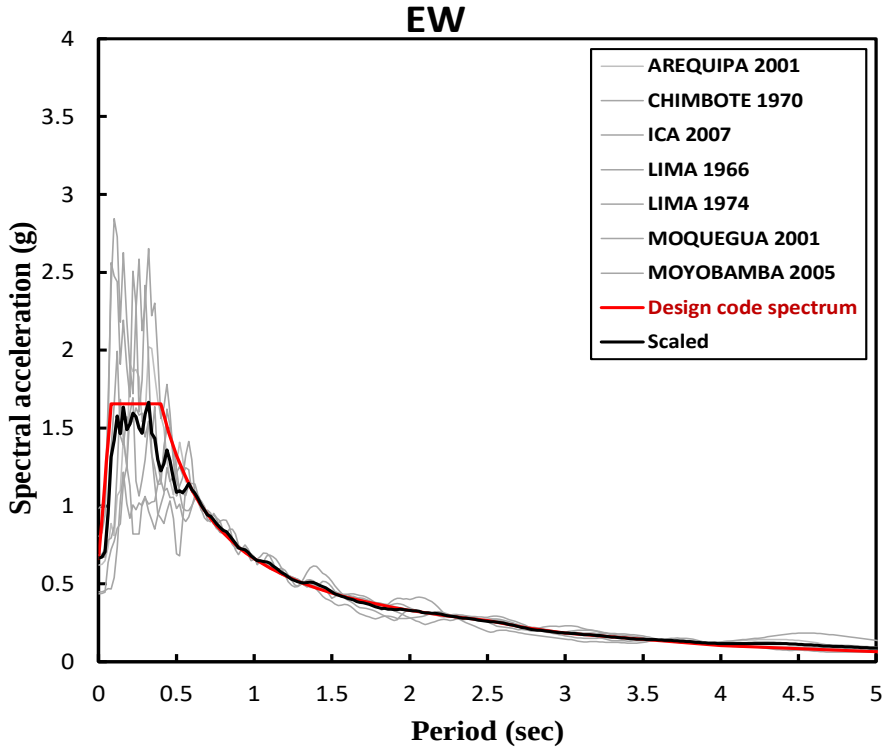

Figure 12. Acceleration spectra scaled EW

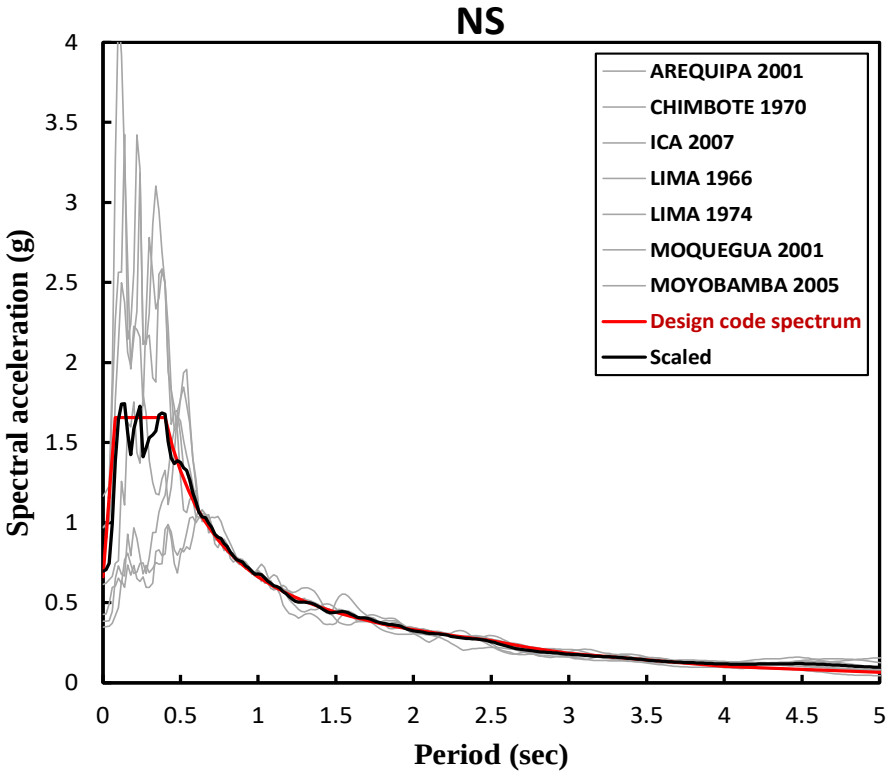

Figure 13. Acceleration spectra scaled NS

2.8. Non-linear Time History Analysis (FNA)

The fast nonlinear analysis (FNA) is a tool used in the ETABS program as a modal analysis method to evaluate the dynamic and static behaviour of linear and nonlinear structural systems, being suitable for the time-history analysis due to its computational formulation, which evaluates the relationship between force and deformation, being suitable for our analysis according to the Bilinear methodology mentioned in Figure 8.

To evaluate the seismic behaviour of the structural models with the base isolation system, we used the non-linear time-history analysis, discarding the spectral modal dynamic model, since the structure is not less than 4 stories or more than 20 m according to the Peruvian Building Regulations, standard E.031 Seismic isolation [22], for which it is necessary to use at least seven sets of ground acceleration records which must be scaled to the defined spectrum, considering the 2 components in the orthogonal directions.

Figure 14 direction X shows the analysis criteria used for the compatible spectrum east-west direction, where the preliminary scaled spectrum was obtained and then in the analysis direction "X" of the record, it was considered east-west at 90%, north-south at 44% simultaneously. The same was done for the 7 pairs of records used.

Figure 14 direction Y shows the analysis criteria used for the compatible spectrum in the north-south direction, where the preliminary scaled spectrum was obtained and then in the "Y" analysis direction of the record, it was considered east-west at 44%, north-south at 90% simultaneously. The same was done for the 7 pairs of records used.

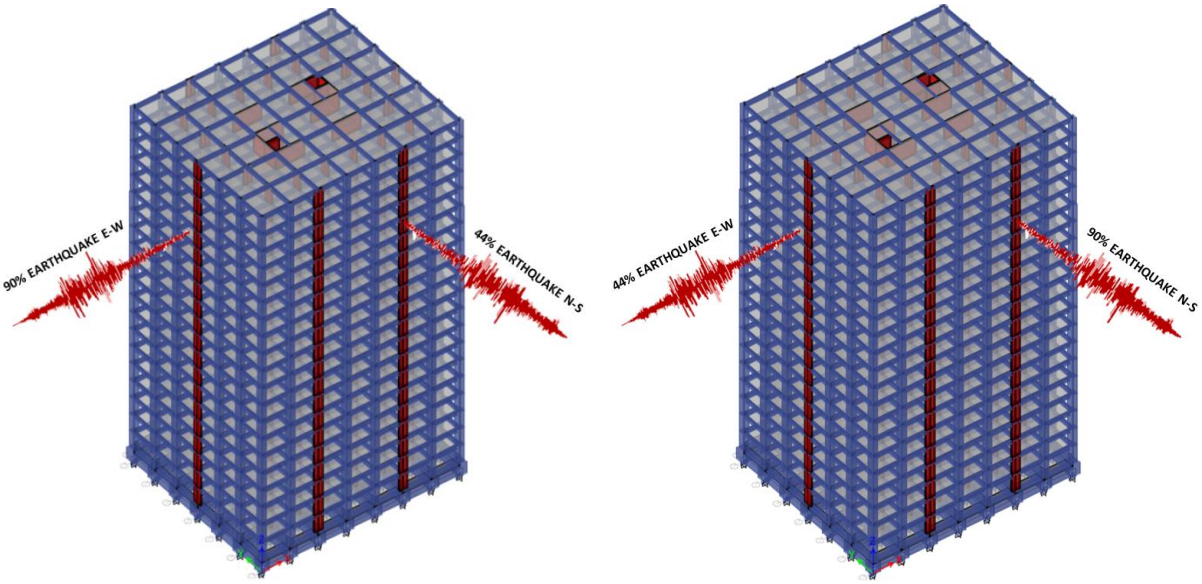

A) Direction “X” B) Direction “Y”

Figure 14. Non-linear time-history analysis considered in the X-direction And Y direction

2.9. Normative Verification Parameters

2.9.1. Vibration Modes

The modes of vibration are determined by stiffness properties and mass distribution which can be simplified by means of a structural model in ETABS [36], which is required by the Peruvian building regulation Norma E.030 Diseño Sismorresistente where it is mentioned, "The modes of vibration must obtain a sum of effective masses greater than 90% of the total mass, for which the first 3 modes of vibration in the direction of analysis are taken into account" [21].

Table 3 shows the vibration modes obtained from the ETABS software, in the standard model without a base isolation system, a period of 1.321 seconds was obtained, predominantly a displacement in "X", being valid to meet a total mass at 90% in mode number 10. In the same way it is validated in the "y" direction having a period of 1. 224 seconds. The period is lower due to the structuring of shear walls in the direction of analysis, while in the Z direction a torsion effect predominates obtaining a period of 1.185 seconds, being verified that the effective masses are greater than 90%. In case the requirement is not met, the number of vibration modes is increased, for the ETABS model was considered 60 modes of vibration in the structure, of which were validated in mode 10 for which reason, only these data have been presented.

Figure 14 shows the standard model with base isolation in which the periods of vibration increased, so in the analysis direction "X" increased by 2.81 times obtaining a period of 3.723 seconds. Another particularity of the isolation system is that the modes of vibration meet the 3 directions of analysis in the fundamental mode 3.

Figure 15 shows the response of the structure of the first 3 fundamental modes of vibration of the standard model with base isolation system, where mode 1 represents the displacement in "X" where there is a 66.43% predominance and 33.21% of displacement in the "Y" direction and without the presence of torsion, in the same way behaves mode 2, where there is 66. 46% of predominance in the "y" direction of analysis while in the "X" direction 33.21%, without the presence of torsion. Finally, the vibration mode 3 shows a predominance of torsion of 99.57% which is adequate according to the analysis carried out in tall buildings [37].

2.9.2. Drift Control

The Peruvian building regulation Norma E.031 Seismic isolation, limits us to the drifts between floors for which a seismic reduction factor (Ra=1) is used, where for the spectral modal analysis it should not exceed 0.0035, while for the time-history analysis considering non-linear force-deformation properties it should not exceed 0.005. This factor is obtained by the difference of displacements between an upper level and the one immediately below divided by their respective analysis height.

2.9.3. Acceleration Control

Accelerations in the structure must be controlled as essential buildings, since the equipment inside the superstructure has to be in operation after a seismic event, for which accelerations less than 0.4g defined as control of interstorey accelerations for structural systems with base seismic isolation are recommended [38].

Table 3. Vibration modes in the structure

Code		Tfixed		Tisolated	
		Mod1	Mod2	Mod1	Mod2
MPAT	FRAMES	1.6137	1.5690	3.8290	3.7370
	WALLS	1.3205	1.2244	3.7225	3.7184
M1	T1	1.0578	1.0180	3.5939	3.5440
	T2	0.9966	0.9664	3.4797	3.4303
	T3	0.9978	0.8886	3.4107	3.3545
M2	T1	1.3870	1.3147	3.7834	3.6830
	T2	1.1707	1.0150	3.4316	3.3570
	T3	0.9666	0.8950	3.0797	3.0560
M3	T1	1.0509	0.9906	3.3260	3.2720
	T2	1.0060	0.9489	3.2580	3.2059
	T3	0.9405	0.8801	3.1217	3.0728
M4	T1	1.2273	1.1878	3.4257	3.3525
	T2	1.1840	1.1590	3.4200	3.3570
	T3	1.1266	1.0750	3.3500	3.2570

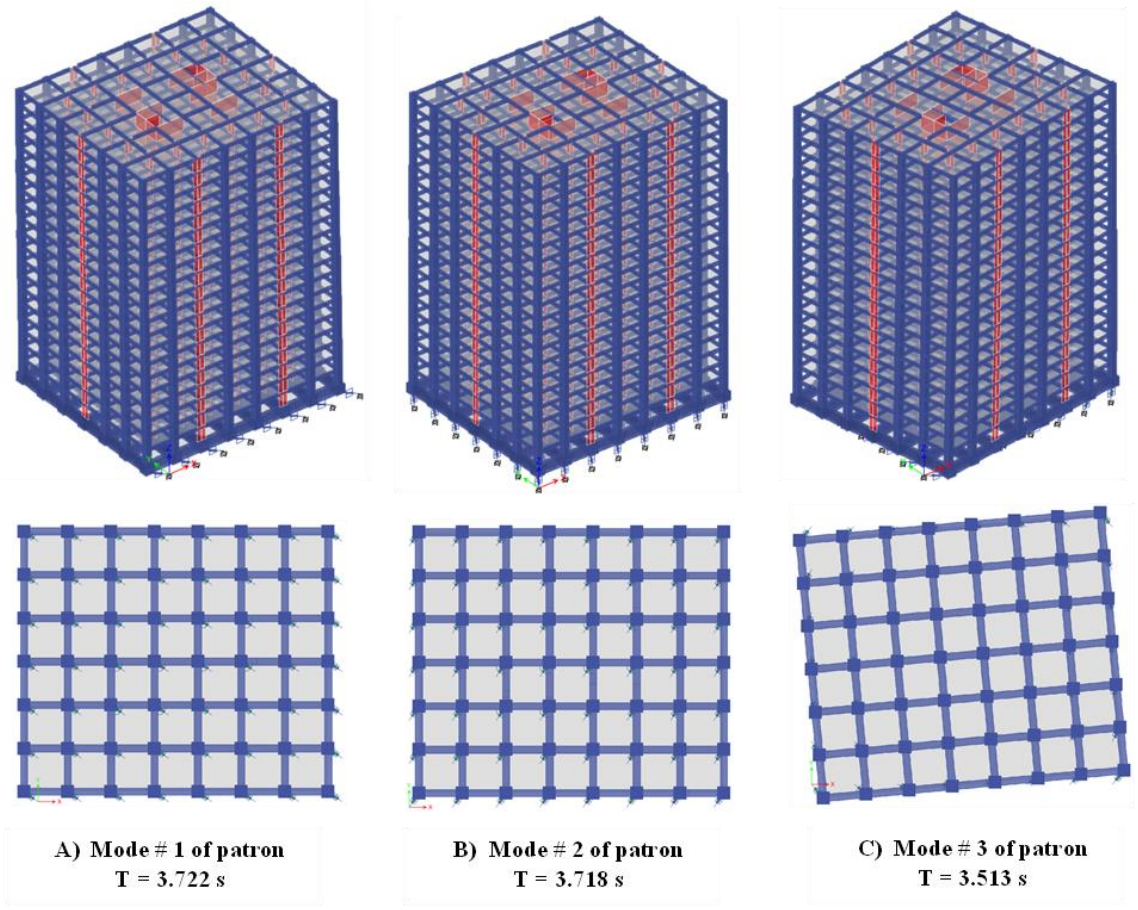

Figure 15. Fundamental modes of vibration of the base-isolated standard structure

3. Results

This section will review the aforementioned models that are structured in the materials section, where the behaviour of the elastomeric and slider isolators is evaluated. The requirements established in the E.031 standard were also verified, such as the control of drifts and accelerations inside the building because they are the main parameters to ensure that a structure will have an immediate occupancy behaviour in the event of a seismic event.

3.1. Location of Insulators

The distribution of the elastomeric isolators and sliders is placed in such a way that their location avoids eccentricity and traction in the structure, thus improving the distribution of forces in the structural elements of the models analysed.

3.1.1. Elastomeric Insulator Properties

Table 4 and Figure 16 show the properties of the elastomeric insulator, therefore, the M4 model has a higher stress because it required a LRB of 1400 mm in diameter to support the stresses caused by the vertical geometric irregularity having a ratio of 1.17, 1.45 and 1.75 respectively. The stresses caused by the vertical geometric irregularity are shown in Table 2. Since the standard model has no irregularity, an LRB of 1000 mm in diameter was required, therefore an increase of 83% was obtained with respect to the model walls, to cover the stresses generated in the foundation. Meanwhile, models M2 and M3 respectively obtained a LRB requirement of 1300 mm in diameter, which represents a 67.44% increase in stresses with respect to the standard WALLS model. Finally, model M1 required an LRB of 1200 mm in diameter, generating an increase of 38.41% in the stress request in relation to the WALLS model, while model frames required an LRB of 1300 mm in diameter to cover the stresses and displacements generated, increasing by 67.44%. It is understood that the most optimal model is the M1 model because at the moment of causing irregularity it only increases by 38.41% unlike the other models which increase by 67.44% and 83% respectively.

3.1.2. Slider Insulator Properties

Table 5 shows the properties of the slider type isolators, where the M4 model is the most stressed and has a geometry requirement of 1250 mm in diameter and a camber of 230 mm, which represent a force of 592.92 kN, followed by the M1 model (584.95kN), M3 (567.73kN), M2 (534.52 kN), which means that the most stressed model is M4 in both the elastomeric isolator and the slider.

Table 4. Properties of elastomeric insulators

Code		Name	Diameter (mm)	Total Height (mm)	Effective plane area (x10 ²mm ²)	Rubber Layer Height (mm)	Rubber Height (mm)	Lead Plug Diameter (mm)	Horizontal Stiffness (kN/m)	Yielding Force (kN)	Initial and post-yield stiffness ratio	After-Yielding Horizontal Stiffness (kN/m)
MPAT	FRAMES	LRB1	1300	376.90	12893.00	8.70	200.00	220.00	3573.84	328.06	13.00	2490.58
	WALLS	LRB2	1000	400.60	7627.00	6.70	200.00	170.00	2120.87	195.92	13.00	1473.93
M1	T1-T2-T3	LRB1	1200	385.60	10996.00	8.00	200.00	200.00	3016.78	271.18	13.00	2121.34
		LRB2	850	413.10	5521.00	5.70	200.00	140.00	1502.63	132.83	13.00	1064.03
M2	T1-T2-T3	LRB1	1300	376.90	12893.00	8.70	200.00	220.00	3573.84	328.06	13.00	2490.58
		LRB2	1000.00	400.60	7627.00	6.70	200.00	170.00	2120.87	195.92	13.00	1473.93
M3	T1-T2-T3	LRB1	1300.00	376.90	12893.00	8.70	200.00	220.00	3573.84	328.06	13.00	2490.58
		LRB2	850.00	413.10	5521.00	5.70	200.00	140.00	1502.63	132.83	13.00	1064.03
M4	T1-T2-T3	LRB1	1400.00	515.50	14978.00	9.50	200.00	230.00	4070.19	358.61	13.00	2886.05
		LRB2	1100.00	390.20	9220.00	7.40	200.00	190.00	2592.28	244.69	13.00	1784.33

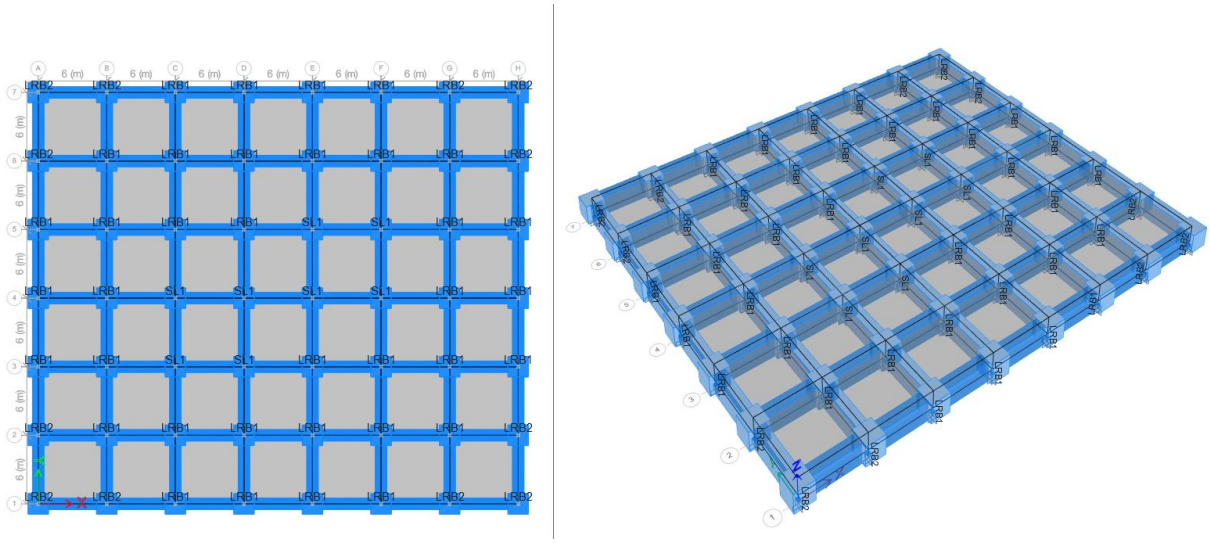

Figure 16. Location of the LRB and Slider insulators

Table 5. Slider insulator properties

Code		Name	Diameter (mm)	Total Height (mm)	Horizontal Stiffness (kN/m)	Yielding Force (kN)
MPAT	FRAMES	SL	1200.00	225.00	2156.96	602.98
	WALLS	SL	1200.00	225.00	2156.96	602.98
M1	T1	SL	1200.00	225.00	2091.81	584.77
	T2	SL	1200.00	215.00	2092.46	584.95
	T3	SL	1150.00	215.00	2012.44	562.58
M2	T1	SL	1200.00	225.00	1912.05	534.52
	T2	SL	1100.00	212.00	1780.82	497.83
	T3	SL	1100.00	212.00	1554.74	434.63
M3	T1	SL	1200.00	225.00	2030.88	567.73
	T2	SL	1200.00	225.00	2045.86	571.92
	T3	SL	1100.00	212.00	1711.01	478.31
M4	T1	SL	1250.00	230.00	2120.96	592.92
	T2	SL	1200.00	225.00	2114.76	591.18
	T3	SL	1200.00	225.00	1993.37	557.25

3.1.3. Tensions in the Insulation System

Table 6 shows the load combinations for the analysis where the minimum and maximum averages of the vertical load applied to each insulator have been calculated according to equations (3), (4), (5), in the same way it has to be verified that there are no tractions in the LRB and Slider insulators, because it represents that there will be a brittle failure of the element by traction.

Table 6. Design load combinations

Code		Name	Diameter (mm)	N °	Pmax	Pserv	Pmin
MPAT	FRAMES WALLS	LRB1	1300.00	44.00	1817.48	964.29	42.12
		LRB2	1000.00	4.00	732.95	348.73	11.10
		SL	1200.00	8.00	3969.92	1929.10	119.60
M1	T1	LRB1	1200.00	33.00	1768.28	976.00	37.56
		LRB2	850.00	15.00	850.37	410.34	8.27
		SL	1200.00	8.00	3904.06	1986.98	194.15
	T2	LRB1	1200.00	36.00	1756.75	952.82	10.31
		LRB2	850.00	12.00	789.36	381.17	-3.67
		SL	1200.00	8.00	3922.76	1987.60	214.59
	T3	LRB1	1200.00	39.00	1710.67	924.70	13.17
		LRB2	850.00	9.00	717.77	359.06	6.74
		SL	1150.00	8.00	3801.87	1911.59	269.92
M2	T1	LRB1	1300.00	36.00	1928.32	1116.09	19.59
		LRB2	1000.00	12.00	1544.55	734.04	42.01
		SL	1200.00	8.00	3932.16	1816.23	26.44
	T2	LRB1	1300.00	36.00	2006.39	1056.76	33.98
		LRB2	1000.00	12.00	1288.69	598.00	-4.95
		SL	1100.00	8.00	3404.85	1691.57	89.31
	T3	LRB1	1300.00	36.00	1825.87	877.77	-138.72
		LRB2	1000.00	12.00	837.92	392.22	4.97
		SL	1100.00	8.00	3164.55	1476.82	-52.30
M3	T1	LRB1	1300.00	36.00	1817.48	964.29	42.12
		LRB2	850.00	12.00	732.95	348.73	11.10
		SL	1200.00	8.00	3969.92	1929.10	119.60
	T2	LRB1	1300.00	34.00	1781.01	969.49	47.22
		LRB2	850.00	14.00	732.11	360.72	9.87
		SL	1200.00	8.00	3890.44	1943.34	49.16
	T3	LRB1	1300.00	36.00	1539.90	850.49	50.90
		LRB2	850.00	12.00	652.30	319.07	27.93
		SL	1100.00	8.00	3324.47	1625.26	60.32
M4	T1	LRB1	1400.00	38.00	2268.82	1168.73	-111.92
		LRB2	1100.00	10.00	1334.87	680.49	-43.10
		SL	1250.00	8.00	4490.87	2014.67	28.27
	T2	LRB1	1400.00	27.00	2247.20	1158.05	-112.78
		LRB2	1100.00	21.00	1517.44	781.62	-14.95
		SL	1200.00	8.00	4146.30	2008.78	23.29
	T3	LRB1	1400.00	24.00	2127.65	1137.31	-21.37
		LRB2	1100.00	24.00	1379.39	670.90	-6.89
		SL	1200.00	8.00	3976.85	1893.47	-27.21

3.2. Behaviour of the Structure

3.2.1. Displacement in the Base Isolation System

Figure 17 shows the behaviour of the displacements from level 0 to 20, also showing the models analysed M1, M2, M3, M4 and MPAT; the graph "Model M1" which has a red line represented by M1T1 presents a displacement of 0.2823 m at the base greater than M1T2, M1T3, MPAT, while at level 20 what shows a greater displacement is M1T3 with a displacement of 0.3216 m compared to the standard model that has a displacement of 0. 3118 m, which would represent an increase in the displacement of 3.14 % being greater than M1T1, M1T2, MPAT. It means that the models with a not so critical irregularity present greater displacements in the base, however the model that had a more pronounced vertical geometric irregularity being M1T3 greater, presented a greater displacement at the last level but in the base, it presents a smaller displacement in model M1. In the graph "Model M2, Model 3, Model 4" in Figure 16, it can be seen that there is a predominance of the MPAT model in the displacement from the base of 0.2794 m and at level 20 of 0.3118 m, this is coherent because the model has a greater mass than M2, M3, M4 that present irregularities and less mass respectively in each of other models. The researchers highlight that the displacements in the building are not affected by more than 3.14% in the 4 models presented, since only in the M1T1 model does it exceed the standard model, while in the M2T3 model it represents 98.68%, M3T3 97.69%, M4T3 96.92% of the displacement with respect to the standard model, M3T3 97.69% and M4T3 96.92%. 92% of the displacement with respect to the standard model, being lower, which indicates these data that the irregularity did not affect the displacement at the upper levels despite the fact that irregularity modifications were made in the different models presented, so this item does not affect this irregularity.

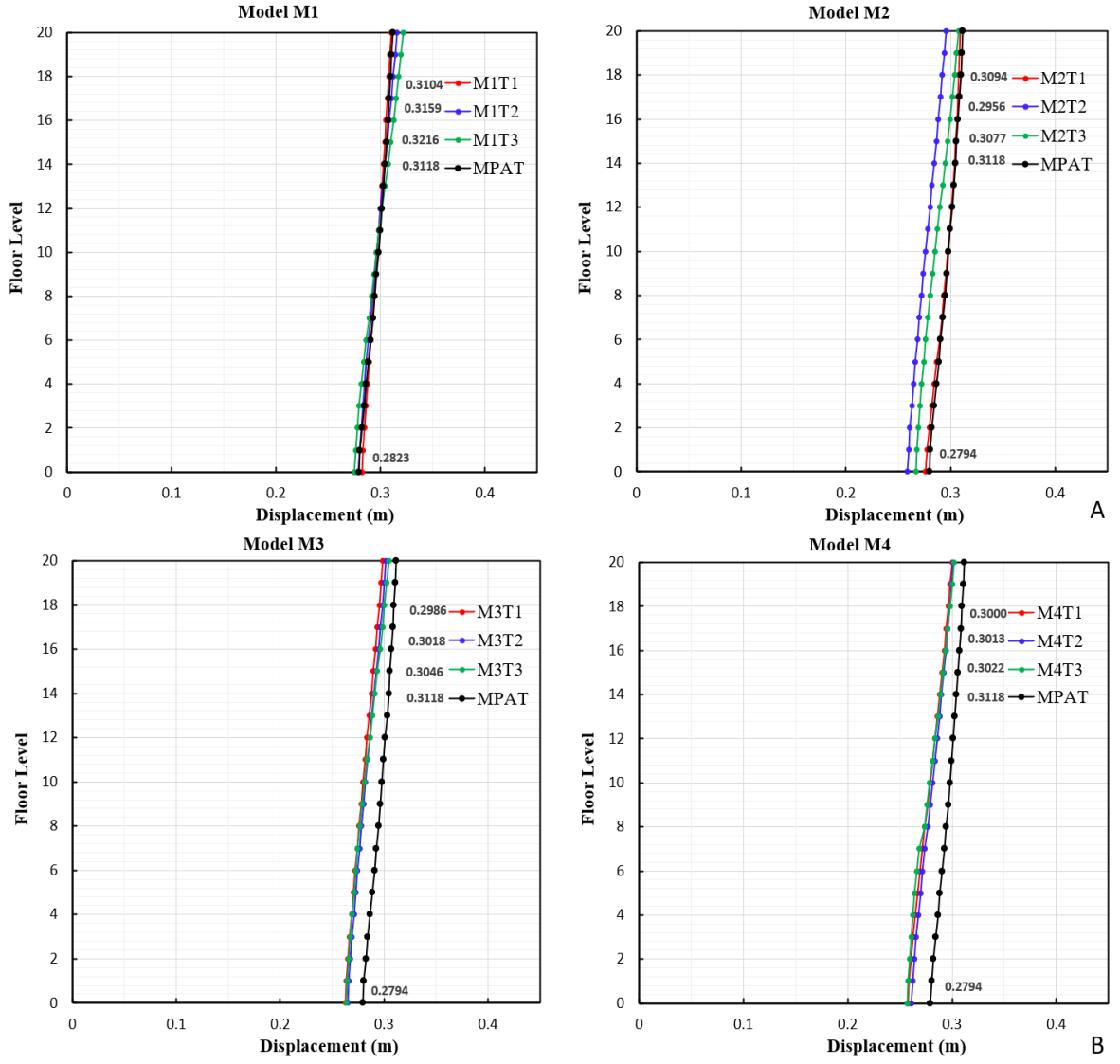

Figure 17. Displacement per level in structure part A and B

3.2.2. Drifts

Figure 18 shows the drifts between floors, which is one of the verification parameters that establishes the suitability of a structure; the established limit is 0.35%. On the other hand, none of the models exceeds this limit. In this way, a comparison of the MPAT and M1T3, M2T3, M3T3 and M4T3 models was carried out, synthesising the information. The type 3 model has a predominance of interstorey drift compared to the other models. Level 20 was used to evaluate the increase of the drift with respect to the standard model, then the model M1T3 increased its drift by 37.72%, M2T3 by 54.53%, M3T3 by 47.11%, M4T3 by 56.75%, so it can be seen that the model M4T3 generates a greater effort to the structure because when there is a greater displacement in the structure. The internal elements will demand an increase in the longitudinal and transverse reinforcement.

Additionally, it is shown in the M1 model that the MPAT has a greater drift behaviour until floor 10 compared to other models with irregularity, but after level 10 the M1T2 model presents an increase in the drift and also the M1T3, while the M1T1 model remains below the MPAT drift until floor 16 where it just presents a behaviour of increased drift. This is reflected because the participatory masses become flexible as the levels increase, presenting this behaviour of drift change in the upper floors.

3.2.3. Accelerations

Figure 19 shows the accelerations of the models analysed. The MPAT model was verified as complying with the maximum permitted acceleration of 0.4g. In model 1, M1T1, M1T2 and M1T3 do not comply with the maximum permitted acceleration limit of standard E.031, with M1T3 showing the highest acceleration of 58.04% with respect to MPAT, while in model M2 it can be seen that M2T1 exceeded the maximum permitted acceleration limit (0.4g) by 0.175%. On the other hand, M2T2 and M2T3 did not comply with this requirement because M2T3 presented an increase with respect to the standard model by 60.63%. Model M3 and M4 do not comply with the maximum permitted acceleration, likewise M3T3 had an increase in acceleration of 44.91% and M4T3 58.55% with respect to the standard model, in short the model that had a greater increase compared to the rest is M2T3 in contrast to model M2T1 which presented a lower acceleration.

3.2.4. Energy Dissipated by the Insulator

Figure 20 shows the M4T3 model of the seismic behaviour of Arequipa 2001, and the analysis carried out in the east-west direction. Also, on the abscissa axis is the time in seconds and on the ordinate the energy in tonf.m; where the kinetic energy, potential energy, energy dissipated by the building, energy taken by the isolators, input energy after 80 seconds were considered. The total energy input is 6675.2932 tonf.m and 6197.4678 tonf.m assumed by the isolators, in effect 92.84% of the energy dissipated by the isolators in the building; being the most overstressed model according to the parameters evaluated in the corresponding items of accelerations and drifts.

The isolators are one of the elements that help to dissipate energy in large quantities, on the other hand, the building itself with its structural components made up of beams, columns, reinforced concrete walls, provides an energy dissipation after 80 seconds of 428.4098 tonf.m, which represents 6. 42%, while the kinetic component can be disregarded because it only has an energy of 0.4 tonf.m and a potential energy of 48.15 tonf.m representing 0.7% compared to the energy entering the building, then the last 2 components can not be considered because their contribution to the dissipation system is negligible unlike the base isolation system.

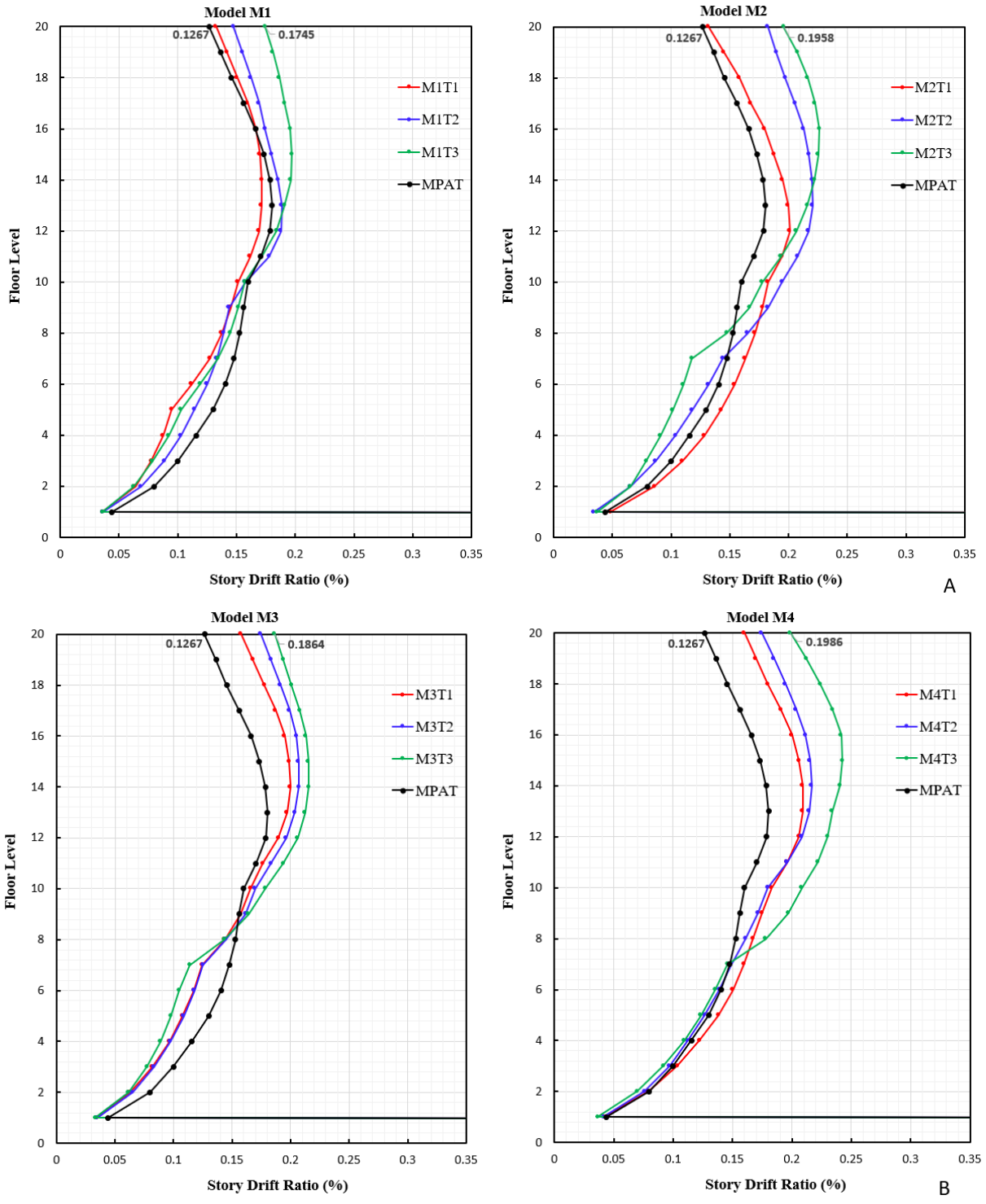

Figure 18. Floor-to-floor drifts per level in structure part A and B

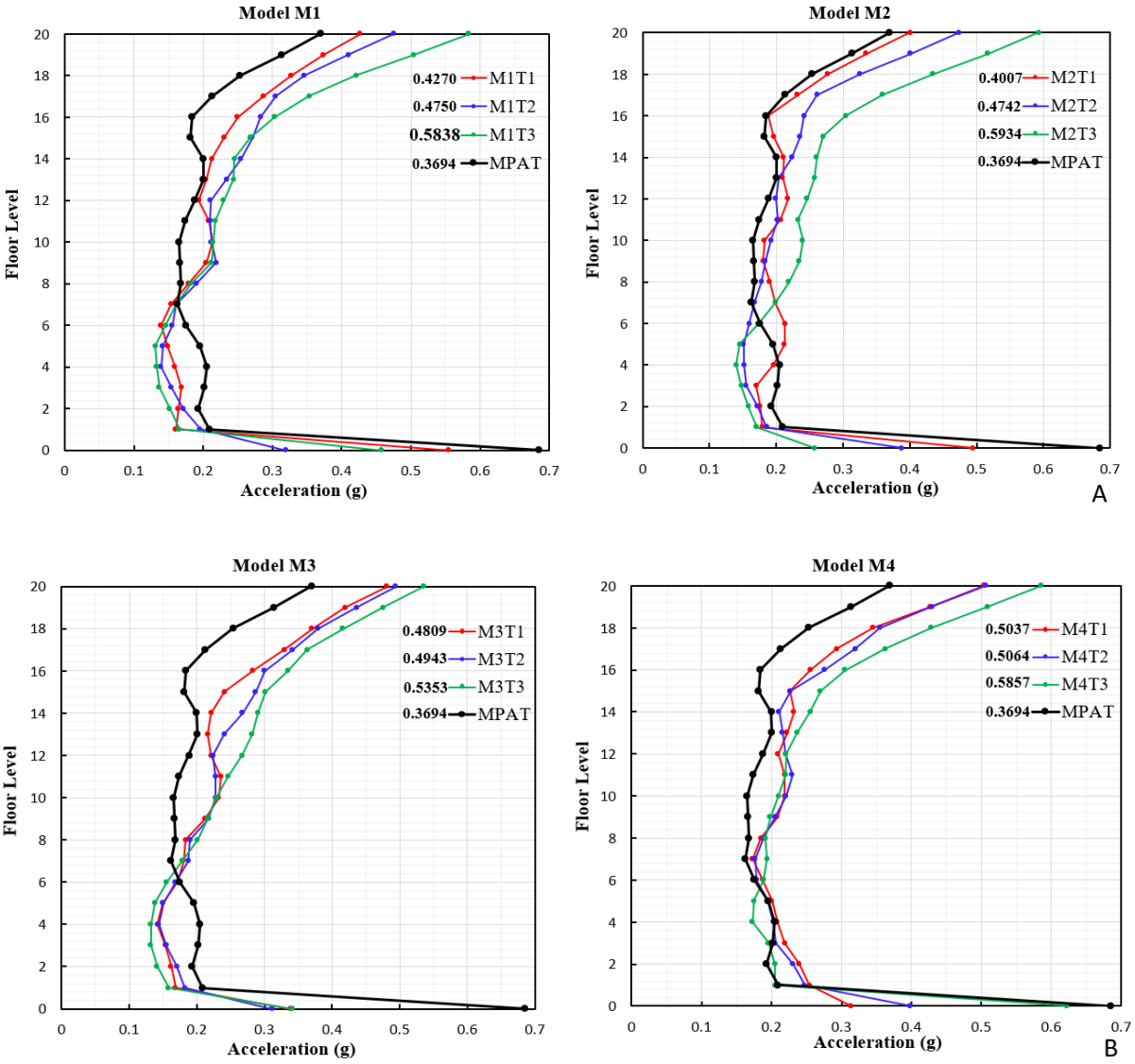

Figure 19. Accelerations by level in structure part A and B

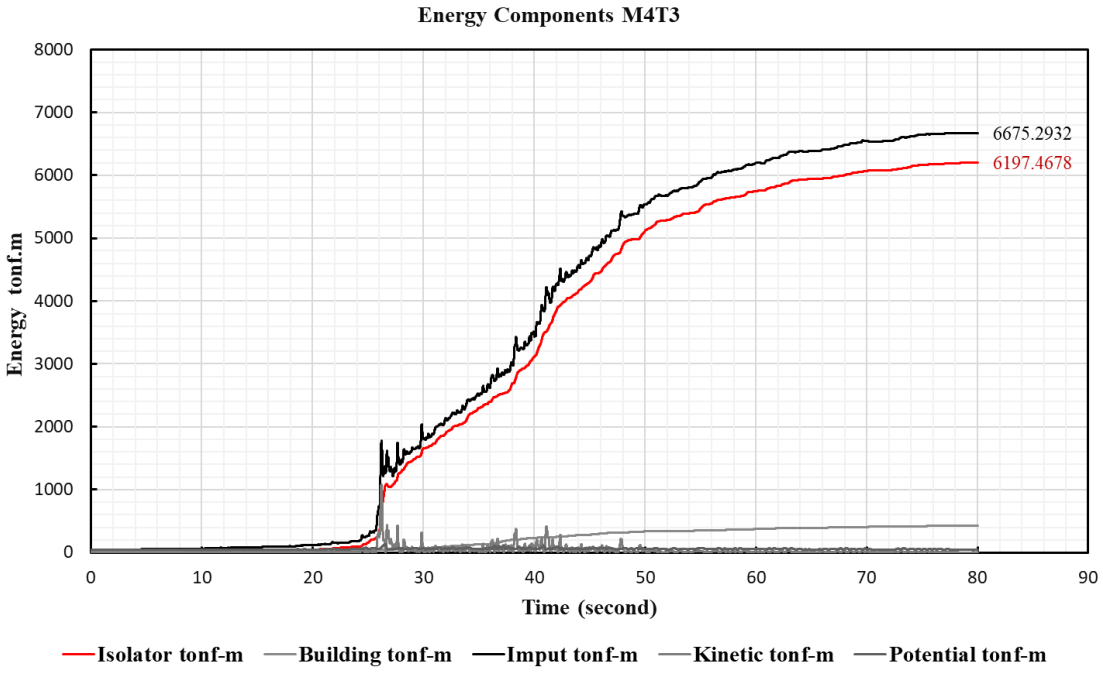

Figure 20. Fundamental modes of vibration of the base-isolated standard structure

4. Discussions

4.1. Effectiveness of the Isolation System

The study by A. Qahir Darwish and M. Bhandari [26] indicates that isolation systems can reduce the seismic response in the range of 50% to 60%, with energy dissipation up to 92.84% using LRB isolators and sliders.

In contrast, the study by I. Mansouri et al [30] highlights that as the percentage of damping increases, the drift decreases, suggesting an improvement in structural performance. This implies that isolation systems can be effective in reducing the seismic response by improving the dynamic behavior of the structure.

4.2. Variations in Structural Periods

The study by M. El-Assaly et al [29] observes that the periods in irregular 20-story structures can be up to 3.54 times greater than that of an unisolated structure. This increase is mainly attributed to the higher seismic mass and the difference in the number of levels.

On the other hand, the study by I. Mansouri et al [30] points out that when the structure is equipped with laminated rubber base (LRB) isolation systems, the periods increase. This observation is consistent with the theory that the increase in periods may be related to the introduction of damping systems, which could indicate a reduction in the effective stiffness of the structure.

4.3. Reduction of Seismic Liability of the Superstructure

The study by A. Qahir Darwish and M. Bhandari [26] shows that the use of isolation systems can transfer the seismic liability to the isolation system, thus reducing the seismic liability of the superstructure to 7.16%. This implies a potential reduction in the steel requirement in the structural parts.

However, the study by I. Mansouri et al. [30] also highlights that isolated structures have a lower probability of damage compared to fixed base structures, suggesting that the introduction of isolation systems can significantly improve the ability of the structure to resist seismic loads without experiencing significant damage.

In summary, although there are differences in the specific results among the studies, all agree that isolation systems can be effective in reducing the seismic response and improving the structural performance of buildings. The choice of the type of isolation system and its impact on structural periods and seismic load distribution may vary depending on the specific characteristics of the structure and the seismic environment.

5. Conclusions

The 4 models analysed against the standard model that provided important data, such as the displacement of the insulation system where it was noted that the M1T1 model presented a greater displacement in the base insulation zone compared to the M1T2, M1T3 and MPAT models, but the models with more pronounced irregularities at the last level, only the M1T3 model had a displacement greater than 3. 14% compared to the standard model without irregularities, while compared to other models the regular isolated system presents a greater displacement of 0.3118m,

the M2T2 model presented a better behaviour in the displacements per floor.

On the other hand, in the evaluation of inter-floor drifts the researchers highlighted that in model M1 the standard model has greater drifts compared to models M1T1, M1T2, M1T3, only up to level 10, but after that level the models M1T2, M1T3 present an increase in their drifts greater than the standard model. This is due to the change of geometry in the upper floors. In the analysed models we observe that the models M1T1, M2T1, M3T1, and M4T1 present a better behaviour, but as the irregularity increases in the models T2, T3, T4 the floor drifts increase.

Likewise, in the analysis of accelerations, the MPAT model is the only one that complies with the maximum permitted acceleration of 0.4g, while of the models with irregularity, only the M2T1 model performed better because it only obtained an excess of 0.175% with respect to the acceleration limit. 175% with respect to the acceleration limit, while the M2T3 model was the one that presented a higher acceleration of 60.63% compared to the standard model, but it is worth noting that in all acceleration curves the M1T3, M2T3, M3T3 presented higher accelerations at the last levels of the roof. The type 1 models have a better behaviour in terms of accelerations.

Finally, after the rigorous analysis of the 12 models with irregularity, we could notice that the elastomeric and slider isolators improve the dynamic behaviour in the reduction of drifts and accelerations achieving columns, reinforced concrete walls, beams, which is due to the reduction of the basal shear of the building. This in turn modifies the structuring in tall buildings, but does not completely eliminate the requirement for shear walls. This is because it is a flexible structure and in order to stiffen, these structural elements are necessary. Therefore this gives us to understand that for tall structures it is necessary to place these walls in the central areas to avoid traction in the areas of the edges, because if we place the shear walls on the perimeter our foundation slab to balance this effect would increase, which would not be economical. Then part of this research is to make a proper structuring to avoid overexerting the elements with unnecessary loads, therefore distributing the elements properly will help to have a better behavior to the structure in general.

Consequently, the present work has provided ideas and clarifications to the behaviour of displacements, drifts, accelerations, and energy dissipation of an irregular structure against the use of LRB and Slider type base isolation. Other useful work to be carried out from this research topic is the analysis of structures in tall buildings as they allow to have a better behaviour in isolated structures, as well as part of it we leave to other researchers to analyse the stresses generated in the geometry change zones versus another level.

6. Supplementary Information

A link to one of the models with vertical geometric irregularity is attached, as well as its respective calculation memory for the sizing and verification of the insulators.

Link: https://continentaledupe-my.sharepoint.com/:f:/g/personal/75911754_continental_edu_pe/EjUXgSH6_2NHrAYn-1Tt6C8B-LAyL5ibZ_JMQhvDL4hX3w?e=qDfW7p

REFERENCES

[1] INEI, “Peruvian population will reach 33 million 726 thousand people in 2023 - News - National Institute of Statistics and Informatics - Peruvian State Platform.” Accessed: Oct. 23, 2023. [Online]. Available: https://www.gob.pe/institucion/inei/noticias/795336-poblacion-peruana-alcanzo-los-33-millones-726-mil-personas-en-el-ano-2023

[2] Andina, “Lima has a trend for the construction of vertical buildings - Revista Constructivo.” Accessed: Oct. 23, 2023. [Online]. Available: https://constructivo.com/noticia/lima-tiene-una-tendencia-por-la-construccion-de-edificios-verticales-1615471298

[3] La República, “Earthquake in Peru: what is the Pacific Ring of Fire and what happens if it activates?? EVAT | Respuestas | La República.” Accessed: Oct. 23, 2023. [Online]. Available: https://larepublica.pe/datos-lr/respuestas/2022/05/13/sismo-en-peru-que-es-el-cinturon-de-fuego-del-pacifico-y-que-pasa-si-se-activa-evat

[4] E. C. Kandemir and A. Mortazavi, “Optimization of Seismic Base Isolation System Using a Fuzzy Reinforced Swarm Intelligence,” Advances in Engineering Software, vol. 174, p. 103323, Dec. 2022, doi: 10.1016/J.ADVENGSOFT.2022.103323.

[5] Z. Zhao, Y. Wang, Q. Chen, H. Qiang, and N. Hong, “Enhanced seismic isolation and energy dissipation approach for the aboveground negative-stiffness-based isolated structure with an underground structure,” Tunnelling and Underground Space Technology, vol. 134, p. 105019, Apr. 2023, doi: 10.1016/J.TUST.2023.105019.

[6] S. D. Darshale and N. Shelke, “Seismic Response Control of Vertically Irregular R.C.C. Structure using Base Isolation,” 2016.

[7] F. Akinci, “The aftermath of disaster in urban areas: An evaluation of the 1999 earthquake in Turkey,” Cities, vol. 21, no. 6, pp. 527–536, Dec. 2004, doi: 10.1016/J.CITIES.2004.08.010.

[8] E. P. Popov, “Observations on the Me Mexico earthquake of 19 September 1985,” Eng Struct, vol. 9, no. 2, pp. 74–83, Apr. 1987, doi: 10.1016/0141-0296(87)90001-0.

[9] M. F. Gallegos, G. Araya-Letelier, D. Lopez-Garcia, and P. F. Parra, “Seismic collapse performance of high-rise RC dual system buildings in subduction zones,” Case Studies in Construction Materials, vol. 18, p. e02042, Jul. 2023, doi: 10.1016/J.CSCM.2023.E02042.

[10] J. M. Tinco and J. A. M. Pelaez, “Seismic Isolation Of Hospitals In Peru: a Case Study With Draft Peruvian Code,” NED University Journal of Research, vol. 3, no. Special

Issue on First SACEE'19, p. 225, Jan. 2020, doi: 10.35453/NEDJR-STMECH-2019-0072.

[11] K. Eriksen, M. Mohammed, and C. Coria, "2018 NZSEE Conference 1 Seismic isolation in North and South America".

[12] E. Ozer, M. Inel, and B. T. Cayci, "Seismic Performance Comparison of Fixed and Base-Isolated Models," Iranian Journal of Science and Technology - Transactions of Civil Engineering, vol. 47, no. 2, pp. 1007–1023, Apr. 2023, doi: 10.1007/S40996-022-00936-4.

[13] E. Ozer, M. Inel, and B. T. Cayci, "Seismic behavior of LRB and FPS type isolators considering torsional effects," Structures, vol. 37, pp. 267–283, Mar. 2022, doi: 10.1016/J.ISTRUC.2022.01.011.

[14] F. De Angelis and D. Cancellara, "Dynamic analysis and vulnerability reduction of asymmetric structures: Fixed base vs base isolated system," Compos Struct, vol. 219, pp. 203–220, Jul. 2019, doi: 10.1016/J.COMPSTRUCT.2019.03.059.

[15] D. Cancellara and F. De Angelis, "Dynamic assessment of base isolation systems for irregular in plan structures: Response spectrum analysis vs nonlinear analysis," Compos Struct, vol. 215, pp. 98–115, May 2019, doi: 10.1016/J.COMPSTRUCT.2019.02.013.

[16] F. De Angelis and D. Cancellara, "Dynamic nonlinear analysis of base isolation systems for multi-storey structures," AIMETA 2017 - Proceedings of the 23rd Conference of the Italian Association of Theoretical and Applied Mechanics, vol. 4, pp. 349–359, 2017.

[17] I. Buckle, S. Nagarajaiah, and K. Ferrell, "Stability of Elastomeric Isolation Bearings: Experimental Study," Journal of Structural Engineering, vol. 128, no. 1, pp. 3–11, Jan. 2002, doi: 10.1061/(ASCE)0733-9445(2002)128:1(3).

[18] Z. Li, X. Chen, G. Huang, A. Kareem, and X. Zhou, "Alongwind and crosswind response of friction-pendulum base-isolated high-rise buildings," Eng Struct, vol. 293, Oct. 2023, doi: 10.1016/J.ENGSTRUCT.2023.116564.

[19] Q. Zhou, M. P. Singh, and X. Y. Huang, "Model reduction and optimal parameters of mid-story isolation systems," Eng Struct, vol. 124, pp. 36–48, Oct. 2016, doi: 10.1016/J.ENGSTRUCT.2016.06.011.

[20] Y. Liu, J. Wu, and M. Donà, "Effectiveness of fluid-viscous dampers for improved seismic performance of inter-storey isolated buildings," Eng Struct, vol. 169, pp. 276–292, Aug. 2018, doi: 10.1016/J.ENGSTRUCT.2018.05.031.

[21] R. P. del P. Javier, A. M. P. Juan, and José Luis Amado Traveza ño, Norma E.030 Seismic-resistant design. José Luis Amado Traveza ño, 2020, pp. 1–81. Accessed: Oct. 30, 2023. [Online]. Available: https://drive.google.com/file/d/1W14N6JldWPN8wUZSqWZnUphg6C559bi-/view

[22] L. C. Yessenia, C. C. Alex, A. C. R. Carlos, and E. T. G. Alvaro, Norma E.031 Seismic isolation. Lima: This Technical Standard establishes the minimum requirements for the design and construction of buildings with any type of seismic isolation system, as well as the applicable provisions for the necessary tests to validate the performance of the building…, 2020, pp. 1–48. Accessed: Oct. 30, 2023. [Online]. Available: https://drive.google.com/file/d/1IZ22Z1h3jfZpp4GKdsLLFQ1FIVSUVUso/view

[23] A. Belbachir et al., "Enhancing the Seismic Response of Residential RC Buildings with an Innovative Base Isolation Technique," Sustainability (Switzerland), vol. 15, no. 15, Aug. 2023, doi: 10.3390/SU151511624.

[24] E. C. Kandemir and A. Mortazavi, "Optimization of Seismic Base Isolation System Using a Fuzzy Reinforced Swarm Intelligence," Advances in Engineering Software, vol. 174, p. 103323, Dec. 2022, doi: 10.1016/J.ADVENGSOFT.2022.103323.

[25] D. De Domenico and G. Ricciardi, "Earthquake-resilient design of base isolated buildings with TMD at basement: Application to a case study," Soil Dynamics and Earthquake Engineering, vol. 113, pp. 503–521, Oct. 2018, doi: 10.1016/J.SOILDYN.2018.06.022

[26] A. Qahir Darwish and M. Bhandari, "Seismic response reduction of high rise steel-concrete composite buildings equipped with base isolation system," Mater Today Proc, vol. 59, pp. 516–524, Jan. 2022, doi: 10.1016/J.MATPR.2021.11.560.

[27] A. F. Roberto and S. C. Jenniffer, "Elastomeric and fps based isolators," A. F. Roberto, L. A. Jose, D. Peter, and S. Vinicio, Eds., Ecuador: Centro de investigaciones cientificas, 2018, pp. 1–302. Accessed: Oct. 30, 2023. [Online]. Available: http://repositorio.espe.edu.ec/handle/21000/3005?locale=de

[28] S. D. Darshale and N. Shelke, "Seismic Response Control of Vertically Irregular R.C.C. Structure using Base Isolation," 2016.

[29] M. El-Assaly, M. Abuelmaaty Amin, S. Saad Galalah, and C. Author, "Regular Versus Vertical Irregular R.C Buildings Using Base Isolation," IOSR Journal of Mechanical and Civil Engineering (IOSR-JMCE) e-ISSN, vol. 18, pp. 26–33, doi: 10.9790/1684-1804022633.

[30] I. Mansouri, G. Ghodrati Amiri, J. W. Hu, M. Khoshkalam, S. Soori, and S. Shahbazi, "Seismic fragility estimates of lrb base isolated frames using performance-based design," Shock and Vibration, vol. 2017, 2017, doi: 10.1155/2017/5184790.

[31] F. Saritaş, I. Bedirhanoglu, A. Konak, and M. S. Keskin, "Effect of Seismic Isolation on the Performance of High-Rise Buildings with Torsional Instability," Sustainability (Switzerland), vol. 15, no. 1, Jan. 2023, doi: 10.3390/SU15010036.

[32] Carlos. López Ramírez, Rodrigo. Retamales, Thomas. Kannegiesser, and Trama Impresores), "Seismic protection of structures: seismic isolation and energy dissipation systems." Chilean Chamber of Construction, p. 43, 2012.

[33] A. R. Patricia, "Seismic isolators strength and protection." Accessed: Oct. 30, 2023. [Online]. Available: https://boroschek.files.wordpress.com/2014/09/201409_bit_aislacionsismica.pdf

[34] M. Gümüş and C. Durucan, "Effects of pulse like ground motion records with and without acceleration pulses on the earthquake responses of structures with varying dynamic properties," Structures, vol. 45, pp. 427–436, Nov. 2022, doi: 10.1016/J.ISTRUC.2022.09.042.

[35] R. K. Tiwari and R. Rajesh, "Factorized Hankel optimal singular spectral approach for erratic and noisy seismic

signal denoising," J Appl Geophy, vol. 111, pp. 95–101, Dec. 2014, doi: 10.1016/J.JAPPGEO.2014.09.019.

[36] R. M. Olivera-Perez, T. Leticia Julcarima-Coca, J. R. Ortiz-Zacarias, I. Lucero Quintanilla-Mosquera, S. I. Del Carpio-Ramirez, and J. James Hinostroza-Yucra, "Mechatronic design of a Stewart platform as a base isolator with an active control system," 2022 IEEE 13th Annual Ubiquitous Computing, Electronics and Mobile Communication Conference, UEMCON 2022, pp. 336–341, 2022, doi: 10.1109/UEMCON54665.2022.9965713.

[37] A. Ganesh, C. Vivek Kumar, G. V. V. Satyanarayana, and J. Selwyn Babu, "Comparison of response spectrum and equivalent static analysis for identifying the safest location of floating columns using ETABS in zone IV," low radioactivity techniques 2022 (LRT 2022): Proceedings of the 8th International Workshop on Low Radioactivity Techniques, vol. 2908, p. 040005, Sep. 2023, doi: 10.1063/5.0161103.

[38] V. Zayas, S. Mahin, and M. Constantinou, "Seismic isolation standard for continued functionality", Accessed: Oct. 30, 2023. [Online]. Available: https://goo.gl/h82Fnk